# Spectral slopes and interannual-to-subannual variability ratios


Daniel Amrhein and Alexey Kaplan

Lamont-Doherty Earth Observatory, Columbia University   Palisades, NY  10964

Contact: dea2102@columbia.edu; alexeyk@ldeo.columbia.edu


S5P7

## Introduction

Spectral slope is a statistic that describes the redness of a time series.  It is computed by fitting a line to the plot of log frequency versus log spectral power density.  Spectral slope is of particular use in climatology, as many geophysical time series can be described by power law processes [Wunsch 2003].  A number of publications have suggested broad implications of spectral slope for different time series [e.g., Blender and Fraedrich 2003, Huybers and Curry 2006, Koscielny-Bunde et al. 1998].

In this poster, we show first that the spectral slopes for surface air temperature, sea level pressure, and precipitation computed from months to decades correspond visually and mathematically to a straightforward climatological quantity, namely the log ratio of  interannual to subannual variances. Second, we use the method of empirical orthogonal functions (EOFs) to identify the dominant modes responsible for spatial patterns of spectral slope. Notably, residual patterns after subtracting only a few leading EOFs appear to be dominated by latitudinal variability and land-sea contrast, particularly for precipitation.  Finally, we interpret leading principal components as well-known modes of  interannual variability.

## Development

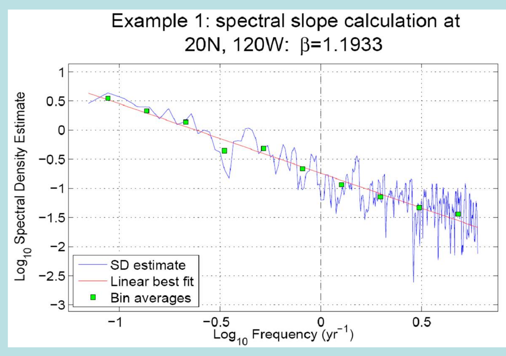


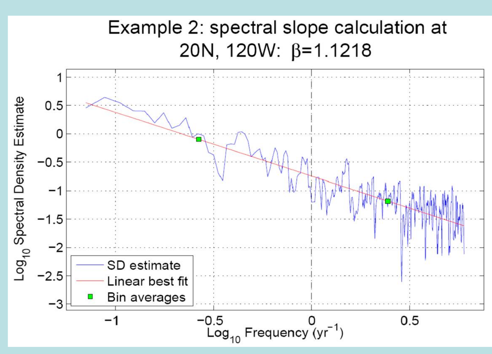


There is clear similarity between the plots of negative spectral slope and the log of the ratio of interannual to subannual variance [see plots this pane]. This similarity is not surprising when one considers the mathematics of spectral slope calculation. We will show that the two quantities are related by a linear transformation.

In general, spectral slope is computed by fitting a linear best-fit line to a plot of log spectral density versus log frequency. Data are binned and averaged before fitting the line into in order to properly weight across the range of frequencies- the density of points is much higher in the upper frequencies [Examples 1 & 2 in this pane], and these frequencies would otherwise dominate the best-fit procedure. One example in the literature uses 10 equally-spaced log-frequency bins [Huybers 2006] [Example 1]. We can adjust the weighting of the spectra by the number of bins that we use.

Consider in particular the case of two bins divided at annual frequency [Example 2]. Then the task of finding the best-fit line is simplified because we are dealing with only two points. These log-frequency values of these points are in the middles of the bins and depend only on the length $l$ of the time series (MATLAB MTM returns power spectral density estimates of length $\frac{l}{2}$). The log-frequency location of the first (interannual) point is given by $M_i = \frac{1}{2}\log_{10}\frac{12}{l}$, and the location of the second (subannual) bin is given by $M_s = \frac{1}{2}\log_{10} 6$ (the six-month frequency is Nyquist frequency for data with one-month temporal resolution). Binned spectral density values are computed by taking the average of the enclosed spectral density points before taking the log to yield physically meaningful units for the bin averages. We can write interannual and subannual bin averages $P_i$ and $P_s$ as

$$P_i = \log_{10}\left[\frac{\sum_1^{np_i} p_i}{np_i}\right] \text{ and } P_s = \log_{10}\left[\frac{\sum_1^{np_s} p_s}{np_s}\right],$$

where $p_i$ and $p_s$ are spectral density values and $np_i$ and $np_s$ are the number of spectral density values in interannual and subannual frequency ranges, respectively. The numbers $np_i$ and $np_s$ also depend only on sample length; $np_i = \frac{l}{12} - 1$ and $np_s = \frac{l}{2} - \frac{l}{12}$.
Letting $\beta$ be spectral slope and expanding, we have

$$\beta = \frac{P_s - P_i}{M_s - M_i} = \frac{\log_{10}\left(\frac{\sum p_s}{\frac{l}{2}-\frac{l}{12}}\right) - \log_{10}\left(\frac{\sum p_i}{\frac{l}{12}-1}\right)}{\frac{1}{2}\log_{10}(6) - \frac{1}{2}\log_{10}\frac{12}{l}}$$

The denominator simplifies to $\frac{1}{2}\log_{10}\frac{l}{2}$, and the numerator can be rewritten as

$$\log_{10}\left[\frac{\sum(p_s)}{\sum(p_i)}\right] + \log_{10}\left[\frac{\frac{l}{12}-1}{\frac{l}{2}-\frac{l}{12}}\right].$$ The entire expression simplifies to

$$-\beta = 2\frac{\log_{10}\left(\frac{\sum p_i}{\sum p_s}\right)}{\log_{10}\frac{l}{2}} - 2\frac{\log_{10}\left(\frac{l-12}{5l}\right)}{\log_{10}\frac{l}{2}}$$

The integral of the spectral density over a given frequency range is equal to the variance of the entire signal accounted for by the frequencies in the range. So $\log_{10}\left[\frac{\sum(p_i)}{\sum(p_s)}\right]$ is equal to the log of the ratio of interannual to subannual variance. This demonstrates that spectral slope is related to the log of the ratio of interannual to subannual variance by a linear transformation that depends only on the length of the time series.

## Data

2m surface air temperature data used in this study are from the NECP-NCAR reanalysis project from 1949-2006 (Kalnay et al. 1996).  Mean sea level pressure data are also from NCEP-NCAR for the same time period (ibid.).  Precipitation data are from the NOAA CPC Merged Analysis of Precipitation (CMAP) monthly climatology, 1979-2006 (Xie and Arkin 1997).  NINO34 index data are from Kaplan (1998).  SOI index data are the differences in standardized seal-level pressure between Tahiti and Darwin. NAO index data are from Hurrell.  IOD index data are from Sontakke et al. 1996.  Indices are truncated to match data set lengths.

## Methods

Spectral slopes are computed by fitting a line via least-squares regression to the log power density spectrum of time series anomalies in log-frequency space.  Power density spectra are estimated via the Thomson multi-taper method using 3 tapers.  To avoid artifacts from the MTM procedure, the lowest three frequencies are discarded.  So that the linear best-fit computation is not dominated by the greater density of high-frequency data points, spectra are binned and averaged in ten equally-spaced log-frequency bins.  Intra-bin averages are computed over the log of the power spectrum values.  This  averaging procedure (discussed in the Development section) rather than the log of the average of the bin average values rather than the average of the log in order to retain a physically meaningful quantity.

Interannual and subannual filtered datasets are computed using a symmetric four-pole low-pass Butterworth filter with half-power point at the annual cycle.   Variances of interannual and subannual regimes are computed by finding the temporal variance at every point of the interannual and subannual datasets, respectively.

EOFs and PCs are computed for the strictly interannual timeseries after inversely scaling the data at every geographical location by the corresponding standard deviation of subannual temperature. With this scaling, data variance at each location becomes precisely the local ratio of interannual to subannual variability (whose logarithm we have connected to the local spectral slope).

Cross-correlations of principal components and climate indices are computed using their linearly detrended values.

## EOF Analysis

Computation of spectral slope, ratio of interannual to subannual variability, and EOF and PC decomposition for 2m surface air temperature, sea level pressure, and precipitation.  EOFs are computed from low-pass-filtered data which are then weighted so that the squared EOF patterns give the variance contribution of each mode to spectral slope.

Residual plots clearly demonstrate reduction in spatial nonuniformities of spectral slope as leading modes are removed.

Cross-correlations with indices show relationships of PCs with known phenomena.

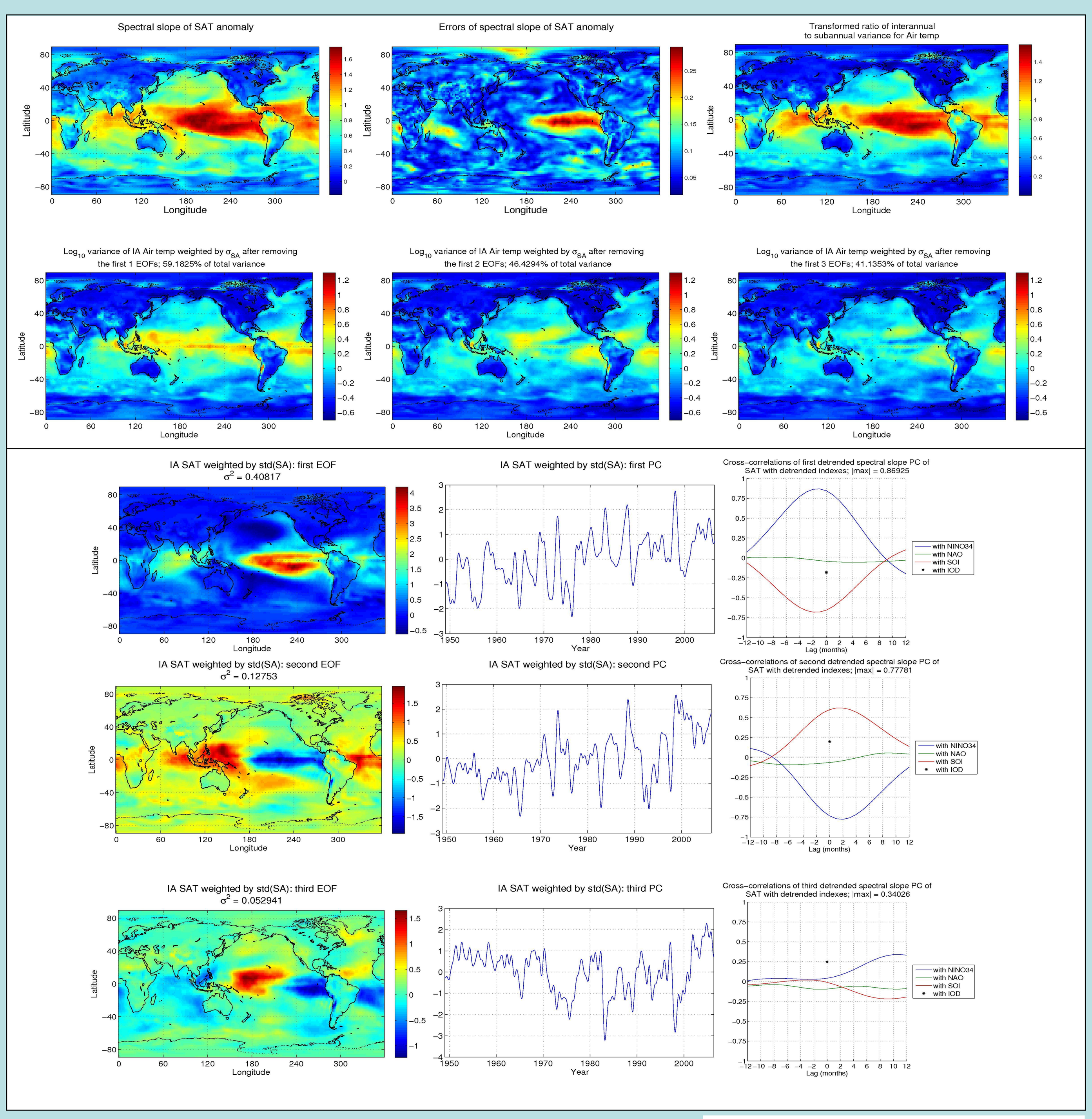


*2m surface air temperature*

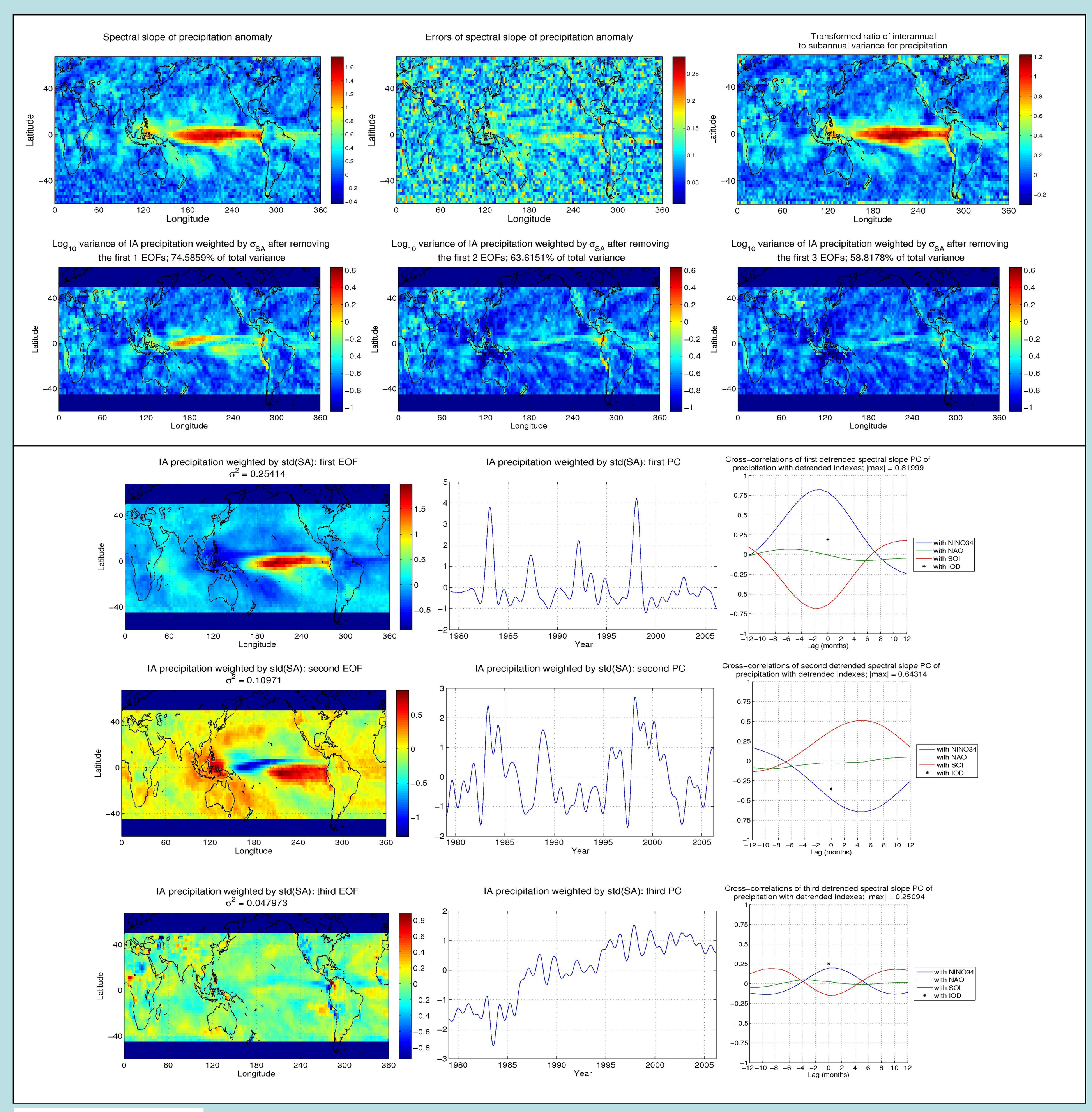


*Precipitation*

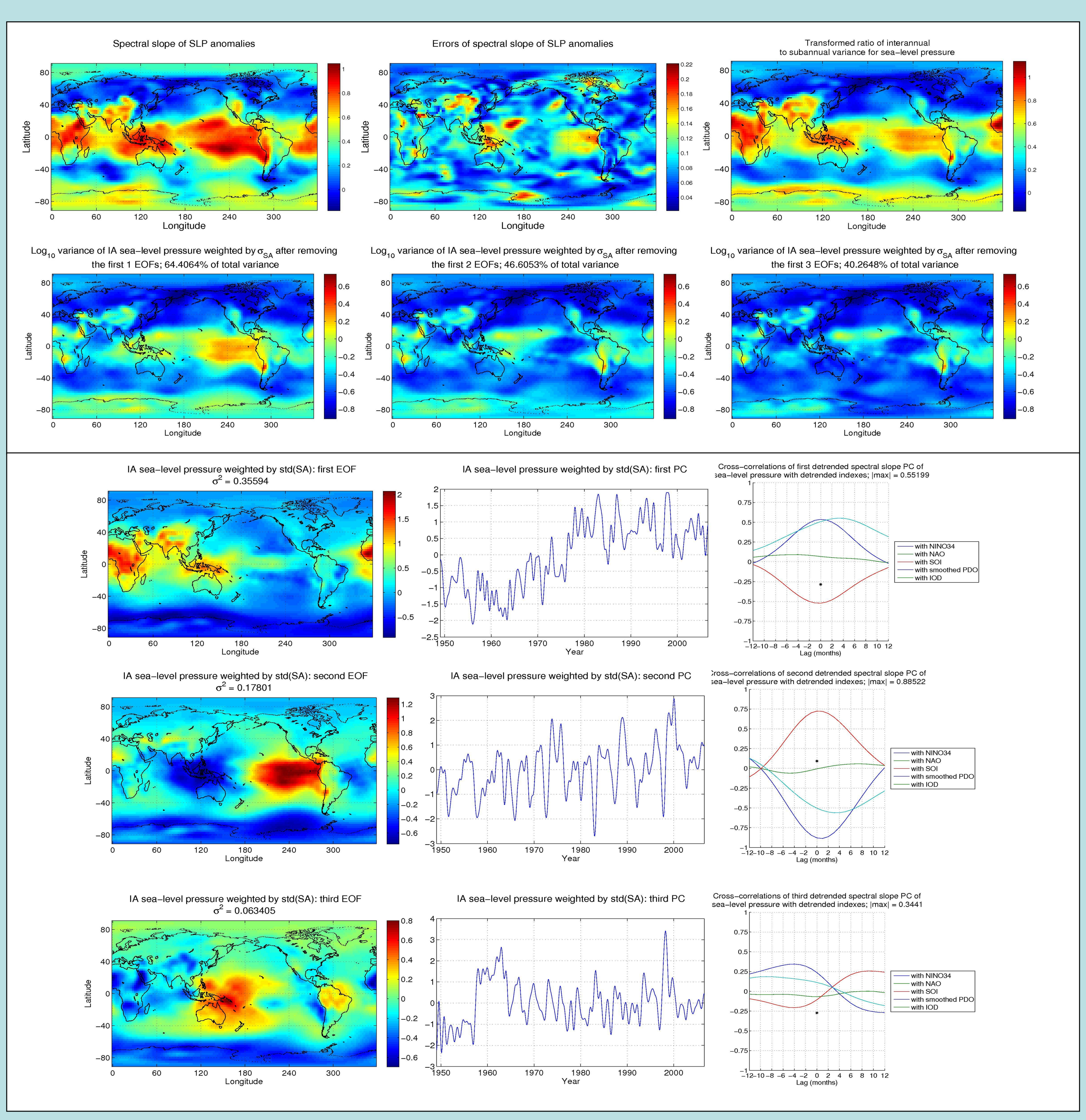


*Sea-level pressure*

## Conclusions

Quantitative connections have been shown between interannual phenomena and the leading principal components of a quantity that is directly related to spectral slope.  We note in particular the importance of ENSO and Pacific Decadal Oscillation variability in determining these quantities.  Spatial variability in spectral slope is drastically reduced by the subtraction of a small number of modes, suggesting that distinguishable dynamical processes and phenomena may be superimposed on a spectral profile which is constant over large regions. Future research will focus on the spectra of residual data after the removal of dominant modes and on developing statistics to characterize nonlinear spectra in a more nuanced way.

## References


Blender, R., and K. Fraedrich. (2003) Long time memory in global warming simulations. *Geophys. Res. Lett*., 30 7(1-4)

Huybers, P., and W. Curry. (2006) Links between annual, Milankovitch, and continum temperature variability. *Nature*, 441 329-332.

Kalnay, E. et al. (1996) The NCEP/NCAR 40-year reanalysis project. *Bull. Am. Metorol. Soc*., 77 437-471.

Kaplan, A., M. Cane, Y. Kushnir, A. Clement, M. Blumenthal, and B. Rajagopalan, Analyses of global sea surface temperature 1856-1991, *Journal of Geophysical Research*, 103, 18,567-18,589, 1998

Koscielny-Bunde et al. (1998) Indication of a Universal Persistence Law Governing Atmospheric Variability. *Phys. Rev. Lett*., 81 729-732.

Sontakke, N.A. , G.B. Pant, and N. Singh 1993, Construction of all-India summer monsoon rainfall series for the period 1844-1991, *J. Clim*., 6, 1807-1811.

Wunsch, C. (2003) The spectral description of climate change including the 100 ky energy. *Climate Dynamics*, 20 353-363.

Xie, P. and P. A. Arkin, 1997: Global precipitation: A 17-year monthly analysis based on gauge observations, satellite estimates, and numerical model outputs. *Bull. Amer. Met. Soc*., **78**, 2539-2558.